13th World Conference on Earthquake Engineering
Vancouver, B.C., Canada
August 1-6, 2004
Paper No. 136

SHAKING TABLE TESTING OF LIQUEFIABLE GROUND IMPROVED BY MULTI-LAYER SOLID

Takahiro KISHISHITA[1], Yoichi YAMAMOTO[2], Naoki TAKAHASHI[3], Fusanori MIURA[4], Masayuki HYODO[5], and Norimasa YOSHIMOTO[6],

SUMMARY

In this study, a series of shaking table tests was conducted under various improvement rates to investigate on the effect of the multi-layer soil improvement method. The multi-layer soil improvement method involves placing multiple plate-like layers of improved soil in a liquefiable layer. As a result, it was found that the multi-layer soil improvement was effective for attenuating seismic motions and repression of settlement.

INTRODUCTION

Due to extensive damage caused by softening and liquefaction of the ground during an earthquake, most soil improvement as measures against liquefaction is intended for elimination of liquefaction. On the other hand, liquefaction can reduce damage and casualties by serving as a base isolation layer for superstructures owing to its ground-motion-reducing effect by strong non-linearization. For instance, liquefaction of the ground immediately below some structures built on a reclaimed land reportedly had an effect of reducing the damage of the superstructures during the 1995 Hyogoken-Nambu Earthquake[1), 2)]. Noticing this effect, attempts have been made to utilize liquefaction for vibration-damping technology applied to forms of foundation and methods of ground improvement[3) - 6)].

The concept of permitting partial softening and liquefaction of the ground may therefore be advantageous over the methods of eliminating liquefaction from the aspect of cost and the

[1] Associate Research, Fujita Corporation, Kanagawa, Japan, Email: kisisita@fujita.co.jp
[2] Chief researcher, Sumitomo Mitsui Construction, Chiba, Japan, Email: yoichiyamamoto@smcon.co.jp
[3] Researcher, Sumitomo Mitsui Construction, Chiba, Japan, Email: tnaoki@smcon.co.jp
[4] Professor, Yamaguchi University, Yamaguchi, Japan, Email: miura@yamaguchi-u.ac.jp
[5] Professor, Yamaguchi University, Yamaguchi, Japan, Email: hyodo@po.cc.yamaguchi-u.ac.jp
[6] Researcher, Yamaguchi University, Yamaguchi, Japan, Email: nyoshi@yamaguchi-u.ac.jp

inertial force to which the structure is subjected. On the other hand, such a method may pose a problem of limiting the settlement and differential settlement of structures on spread foundations within the permissible ranges. Also, the applicability of such ground improvement techniques to existing structures is a pressing subject to meet the growing need for technologies to maintain and repair existing structures in recent years.

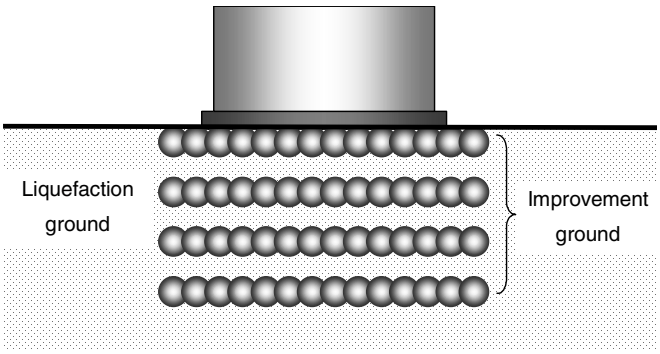

Fig. 1 Concept of multi-layer chemical compaction

Accordingly, the authors devised a form of ground improvement by multi-layer chemical compaction, in which ground is partially compacted to form multiple layers of compacted plates in a liquefiable ground, thereby permitting partial softening and liquefaction to utilize their vibration-damping effect while reducing settlement and differential settlement (Fig. 1). Since chemical grouting is assumed for the ground compaction, it is applicable to grounds under existing structures. The reduced amount of the chemical due to partial co mpaction will also contribute to cost reduction.

In this study, shaking table tests were conducted on model grounds improved by multi-layer chemical compaction with different improvement percentages to investigate the effects of the method in regard to vibration damping and settlement prevention.

OUTLINE OF SHAKING TABLE TESTING

Sample and compacted plates

The sample for ground models is sand from Hamaoka (G_s = 2.699, e_{max} = 0.933, and e_{min} = 0.593). Compacted plates were prepared by pluviating Hamaoka sand onto forms measuring 20 by 20 by 5 cm filled with permanent grout (Permarock)[7] of a water-glass type and cured for 1 week before testing. Table 1 gives the compositions and uniaxial compressive strength of the permanent grout. Figure 2 shows the relationship between the cyclic shear stress ratio, τ_{cyc}/σ'_m, and the number of cycles causing a shear strain with a peak-to-peak amplitude of 5%, N, obtained from undrained cyclic simple shear tests on Hamaoka sand with a relative density of 50% and compacted plates cured for 7 and 28 days. Whereas liquefaction occurred in 100% Hamaoka sand, reaching a strain with a peak-to-peak amplitude of 5%, no liquefaction occurred in the compacted plates. The cyclic strength of the compacted plates was approximately 1.0 in terms of the stress ratio, being significantly higher than unimproved sand.

Test procedure

Shaking table tests were conducted using shear soil tanks measuring 1.2 by 0.8 by 1.0 m in a gravitational force field. Figure 3 shows a schematic of the test model. Measurement was made using accelerometers, piezometers, and strain gauges in the ground, an accelerometer and laser displacement gauge on the superstructure, and accelerometers and laser displacement gauges on the shear frame. The model ground consisted of a liquefiable layer 60 cm in depth on a non-

liquefiable layer 40 cm in depth. The non-liquefiable layer was prepared by pluviating dry sand and then compacting to a relative density of 80% by actuating the shaking table. The liquefiable upper layer was prepared by pluviating dry sand while placing precompacted plates at the specified levels. The initial relative density of the upper layer was approximately 35%. The ground was saturated to the surface by pouring water from the bottom before being subjected to shaking. After saturating the ground, a model structure measuring 20 by 20 by 20 cm simulating a spread foundation building was placed in the center of the ground surface.

White noises with a maximum acceleration of 200 gal (L-1 input) and 400 gal (L-2 input) were applied to each of the model grounds with and without compacted plates. Model grounds containing compacted plates were made with five different improvement percentages (total thickness of compacted plates / depth of liquefiable layer) as shown in Fig. 4. Figure 5 shows the input acceleration waveform with a maximum of 400 gal.

Table 1 Compositions of chemical grout and strength of compacted plates

	Solution name	Volume(ml)
A liquid	ASF silica	60
	AKUTA M	16
	Water	124
B liquid	PR silica	60
	Water	140
Compressive strength	$q_{u7(kPa)}$	120
	$q_{u28(kPa)}$	159

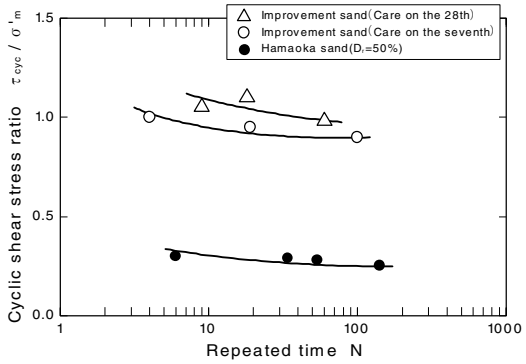

Fig. 2 Relationship between cyclic shear stress ratio and number of cycles

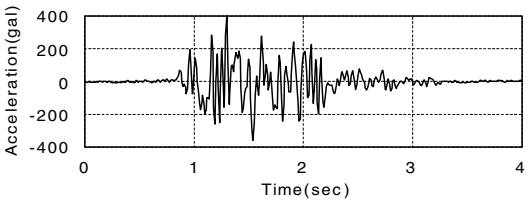

Fig. 5 Input acceleration waveform (L-2)

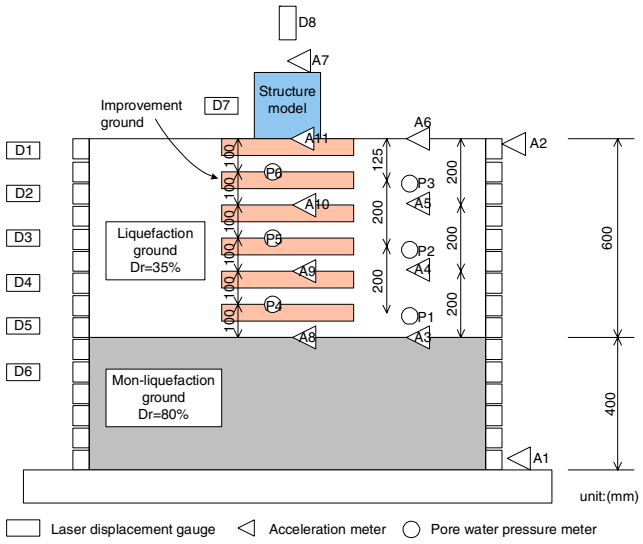

Fig. 3 The outline of a model experiment

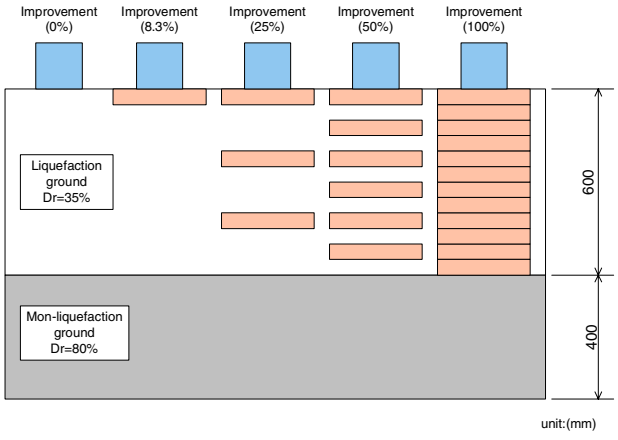

Fig. 4 Experiment cases

RESULTS AND DISCUSSION

Changes in the response values over time

Figure 6 shows the changes in the sensor outputs recorded during L-2 input. The records on the left, center, and right represent the results of models with no improvement, 50% improvement, and 100% improvement, respectively. The first row represents the acceleration responses at the top of the structure (A7). The response acceleration at the top of the structure increases as the improvement percentage increases, while the period of the waveform decreases.

The second row compares the response accelerations at the ground surface (A6, solid line), top of the compacted plate (A11, solid line) and the bottom of the soil tank (A1, dotted line). The response accelerations at the ground surface and top of the compacted plate show similar tendencies as those of the model structure with the same improvement percentage, but reveals significant amplification on the structure in the case of 100% improvement.

The third row compares the horizontal response displacement of the model structure (D7, solid line) and the top of the shear frame (D1, dotted line). The phases of response of the structure and the top of the shear frame are the same in all cases, suggesting no localized changes in the horizontal displacements on the same level of the ground.

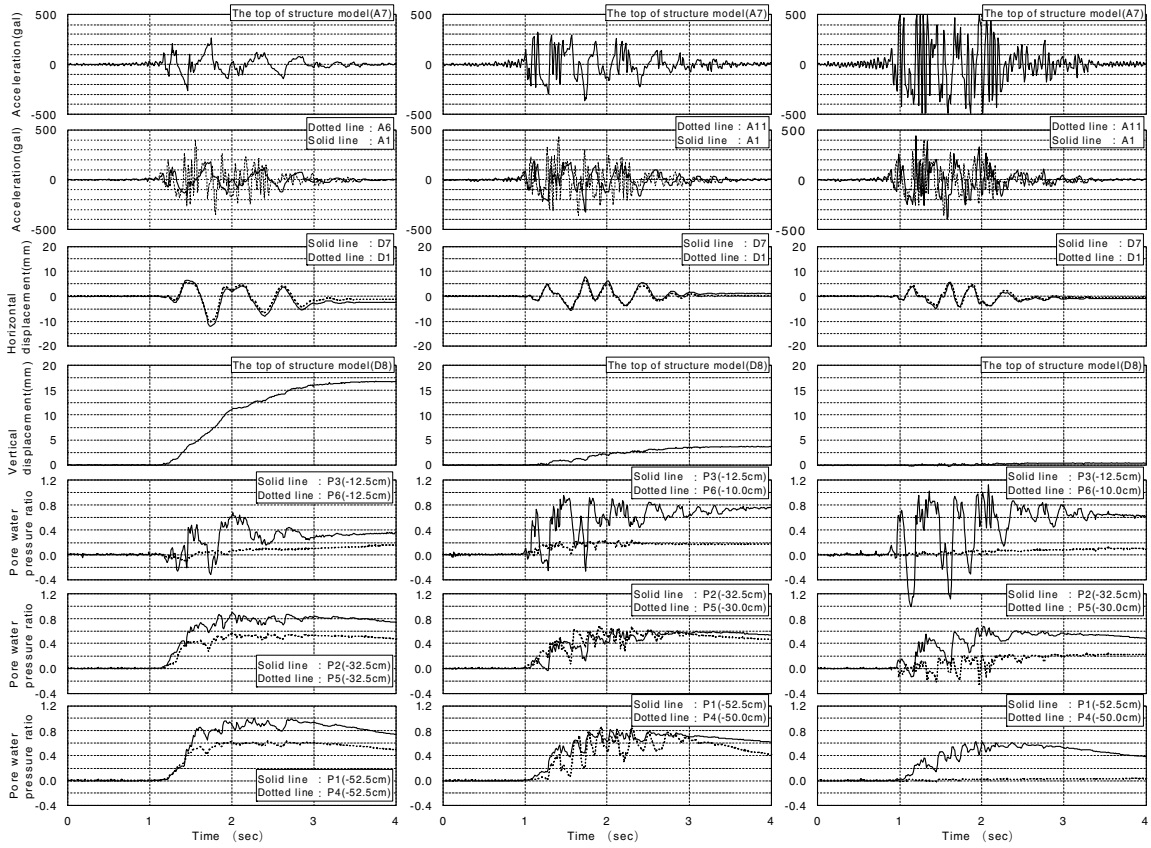

(a) Improvement 0% (b) Improvement 50% (c) Improvement 100%

Fig. 6 The time history response of each sensor (L-2 input)

The fourth row shows the settlement of the model structure. The settlement decreases as the improvement percentage increases. When referring to other response values, the settlement is found to occur mostly during the loading time, while being scarcely found thereafter in the dissipation phase of the pore water pressure.

The fifth to seventh rows compare the excess pore water pressure ratios in the ground nearby (solid line) and the ground under the structure (dotted line). The excess pore water pressure ratios were determined by normalizing the measurements by the effective overburden pressure obtained from a preliminary deadweight analysis. The time-related changes in the measurements at upper nearby ground (P3) show vertical movements corresponding to the phase of horizontal displacement, suggesting the effect of the shear frame on the pore water pressure. The excess pore water pressure ratios in the ground nearby exceeded 0.8 in all cases, indicating liquefaction of the ground. The measurements in the 100% improved ground under the structure show little excess pore water pressure in the improved ground.

Maximum response

Excess pore water pressure profiles

Figure 7 ((a) and (b)) shows the vertical distributions of maximum pore water pressure in the ground nearby and under the structure during the L-2 input ground motion. The maximum excess pore water pressure values in the ground nearby generally show tendencies similar to the results with no improvement (0%) except for a few measuring points, indicating liquefaction of the ground. In regard to the maximum excess pore water pressure in the ground under the structure, the piezometers for 100% improvement were set in the compacted plates, whereas those for partially improved cases were set in the unimproved sand. It is evident that little pore water pressure develops in the compacted plates, as the maximum excess pore water pressure in the 100% improved ground is lower than in other cases. However, the maximum excess pore water pressure of partially improved ground is high, even exceeding the values in the ground

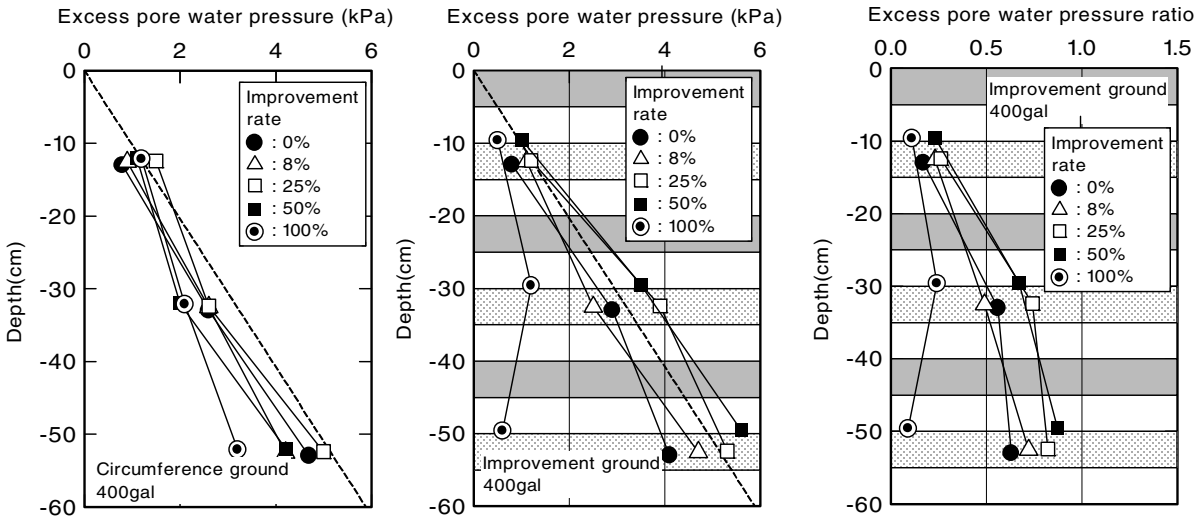

(a) Circumference part (b) Improvement part

Fig. 7 Maximum excess pore water pressure profiles (L-2 input)

Fig. 8 Distribution of maximum excess pore water pressure ratio (L-2 input)

nearby in some cases. This can be attributed to the effect of the increase in the overburden pressure resulting from the presence of a structure with spread foundations, but is considered to be due mainly to the differences in the acceleration responses stated below.

Figure 8 shows the distribution of the maximum excess pore water pressure ratio in the ground under the structure normalized by dividing by the effective overburden pressure determined from a deadweight analysis. This figure reveals that the excess pore water pressure ratio increases as the depth increases, excepting the case of 100% improvement. The upper part is less prone to liquefaction due to the shakedown during the vibration, while being strongly affected by the increase in the overburden pressure resulting from the deadweight of the structure.

Maximum acceleration profiles

Figure 9 (a) and (b) show the vertical distribution of the maximum acceleration during the input ground motion of L-2 in the ground nearby and under the model structure, respectively. The accelerations in the ground nearby are similarly attenuated by the softening/liquefaction of the upper layer (0 to –60 cm from the ground surface) in all cases. However, the acceleration near the ground surface tends to increase as the improvement percentage increases due to the presence of compacted plates. In the ground under the model structure, a tendency for attenuation depending on the improvement percentage is recognized in the upper layer (0 to –60 cm) similarly to the ground nearby. In the case of 100% improvement, however, the acceleration is significantly amplified near the ground surface in contrast to other cases. Whereas the results of surface improvement (8% improvement) tend to coincide with those of no improvement (0% improvement), the results of multi-layer improvement cases of 25% and 50%, though their degrees of reducing the acceleration are low, tend to nearly coincide. These groups characterize the acceleration profiles.

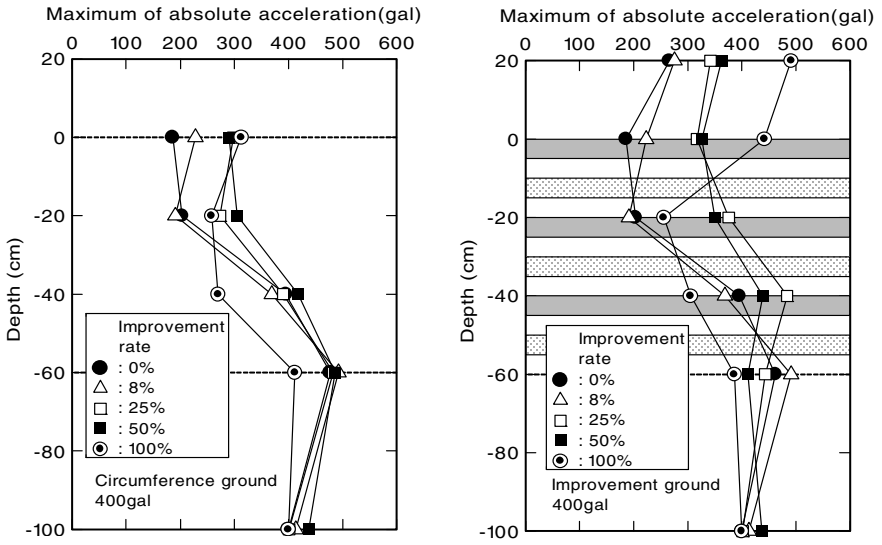

(a) Circumference part (b) Improvement part

Fig. 9 Maximum acceleration profiles (L-2 input)

Relationship between improvement percentage and effect of improvement

Figure 10 shows the magnification of the acceleration on the ground surface in response to an L-2 input ground motion with respect to the bottom of the upper layer (-60 cm) versus the improvement percentage for both the improved ground under the model structure and the ground nearby. The magnification of the response acceleration of the improved ground increases as the improvement percentage increases. Similar tendencies are observed in the ground nearby, though not so evident as in the improved ground. Figure 11 shows the relationship between the amplification ratio of the response acceleration and the improvement percentage in the improved ground under the model structure during the input ground motion of L-2. The amplification ratio of the response acceleration in this figure is determined by normalizing the magnification of the response acceleration shown in Fig. 10 by the magnification of the response acceleration of the unimproved case (0% improvement). This figure reveals that the improvement percentages of 50% and 100% lead to an amplification of 2 times and approximately 3 times, respectively. It is therefore evident that a relatively high vibration-damping effect is achieved by partial improvement permitting partial softening and liquefaction of the ground.

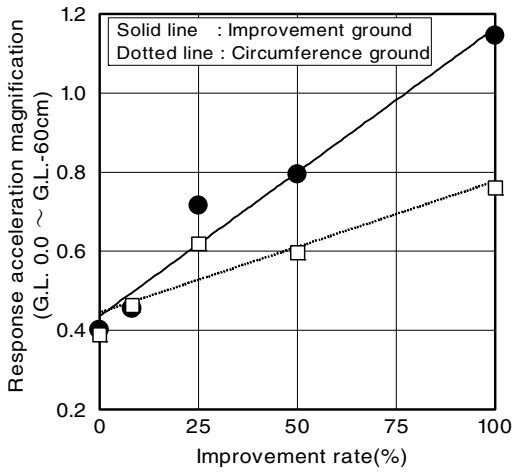

Fig. 10 Relationship between magnification of response acceleration and improvement percentage

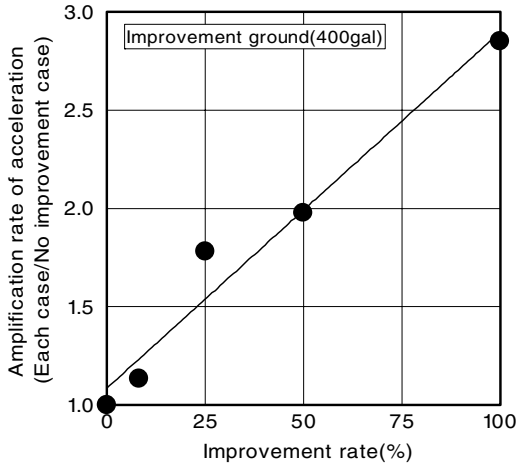

Fig. 11 Relationship between amplification ratio and improvement percentage

Figure 12 shows the relationship between the maximum settlement and the improvement ratio. The settlement is found to decrease as the improvement ratio increases. Since the settlement is less than 1 mm for the 100% improved ground, the compressibility of the chemical-compacted sand is significantly smaller than that of uncompacted ground. It is also found that an increase in the input acceleration level leads to an increase in the settlement greater than the magnification of the acceleration. It should be noted that the actual input acceleration of L-1 and L-2 varies, though the target maximum accelerations are 200 and 400 gal for L-1 and L-2, respectively. The settlement values shown in Fig. 12 were therefore corrected with respect to input accelerations of 200 and 400 gal from the relationship between the input acceleration and the maximum settlement. Figure 13 shows the corrected settlement of improved ground divided by the corrected settlement of unimproved ground versus the improvement percentage. This figure clearly expresses the settlement-inhibiting effect depending on the improvement percentage. The

settlement of the ground with an improvement percentage of 50%, for instance, is reduced to less than 30% of that of unimproved ground (0% improvement), indicating that the settlement-inhibiting effect is greater than the improvement percentage. Since similar relationships are observed for both input accelerations, this type of ground improvement is considered to allow selection of the improvement percentage according to the required level of settlement of the structure.

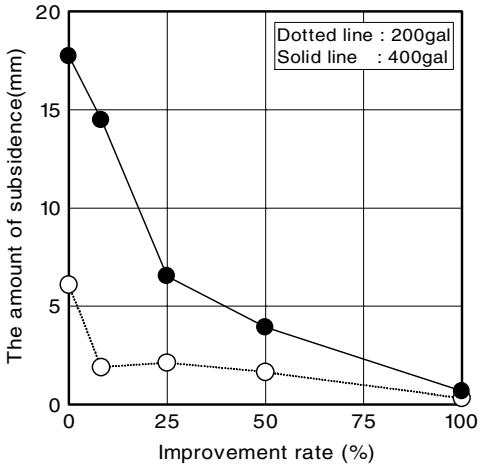

Fig. 12 Relationship between settlement of structure and improvement percentage

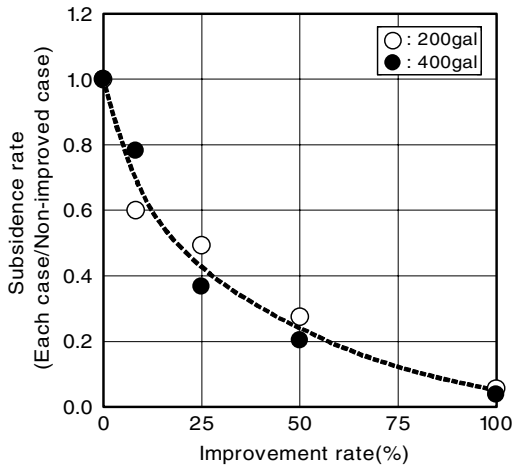

Fig. 13 Relationship between settlement ratio and improvement percentage

CONCLUSIONS

The ground-improving effect of multi-layer chemical compaction was investigated by shaking table testing. As a result, the following were found: Whereas the magnification of the response acceleration increases as the improvement increases, the effectiveness of partial improvement permitting partial softening and liquefaction of the ground is relatively high when compared with full improvement. The relationship between the settlement and the improvement percentage tends to be similar regardless of the level of input acceleration, indicating that the settlement-inhibiting effect of the multi-layer chemical compaction exceeds the improvement percentage.

REFERENCES

1. Hirai Y, Kakurai M, Maruoka M, Yamashita K, Aoki M.” Behavior and evaluation of spread foundations on liquefied reclaimed artificial ground.” The Foundation Engineering & Equipment, Vol.24, No.11, pp.60~66, 1996.
2. Kakurai M, Aoki M, Hirai M, Matano H. “ Investigation of Spread Foundations on Liquefied Man-made Islands” The Japanese Geotechnical Society, Vol.44, No.2, pp.64~66, 1996.
3. Earthquake Engineering Committee, JSCE, “ Guidelines for structural design methods for vibration damping, base isolation and vibration control” 2002.

4. Fukutake K. “ Ground isolation due to liquefaction and its effect on structure (Part2)” PROCEEDINGS OF THE THIRTY-SIXTH JAPAN NATIONAL CONFERENCE ON GEOTECHNICAL ENGINEERING, PP.1735~1736, 2001.
5. Fukutake K. “ Base isolation foundation utilizing nonlinearity of weak ground – focusing on ground base isolation by positive utilization of liquefaction ” The Foundation Engineering & Equipment, Vol.30, No.12, pp.21~28, 2002.
6. Fukutake K. “ Ground Isolation Technique Utilizing Liquefaction Phenomena “The Japanese Geotechnical Society, Vol.51, No.3, pp.31~33, 2003.
7. Yonekura R, Shimada S, “ Mechanism of the permanentness of permanent grout “ Civil Engineering Journal, Vol.40, No.7, pp.99~106, 1999.